Structure of strange baryons

A.J. Buchmann

Institute for Theoretical Physics, University of Tübingen, Auf der Morgenstelle 14, 72076 Tübingen, Germany

Abstract. The charge radii and quadrupole moments of baryons with nonzero strangeness are calculated using a parametrization method based on the symmetries of the strong interaction.

PACS. 14.20.Jn Hyperons – 13.40.Gp Electromagnetic form factors – 11.30.Ly Other internal and higher symmetries

1 Introduction

The discovery of the first strange meson by Rochester and Butler [1] marked the beginning of a new era in subatomic physics. Since then a great deal has been learned about the strong and electroweak interactions of mesons and baryons. However, our knowledge of their spatial structure is still rather limited. In contrast to the N and Δ, which have been investigated with increasing precision [2–4], little is known about the spatial structure of their strange siblings with whom they form the octet and decuplet baryon families. For example, while proton and neutron charge radii were already measured half a century ago [5], a first determination of the Σ^- charge radius has only recently become possible [6]. Up until now, there have been no experiments that pertain to the shape of hyperons [7]. In addition, with respect to theory we are still lacking a thorough understanding of the structure of most hadrons. Various model calculations of hyperon charge radii [8] and quadrupole moments [9] differ considerably in their predictions. The reasons for these differences are often unclear. To gain a better understanding, we investigate to what extent these structural features are determined by the symmetries of the strong interaction.

2 Strong interaction symmetries

Invariance of the strong interaction under SU(2) isospin transformations leads to isospin conservation and the appearance of degenerate hadron multiplets with fixed isospin, such as the pion triplet and nucleon doublet. In the 1950s numerous new meson and baryon isospin multiplets were discovered [10]. The unusually long lifetime of these new particles (fast production but slow decay) was explained by Pais, Gell-Mann, and Nishijima [11] by invoking a new symmetry principle and additive quantum number called 'strangeness'. The latter was assumed to be conserved in strong and electromagnetic interactions (production) but violated in weak interactions (decay), thus explaining the long lifetimes of strange hadrons.

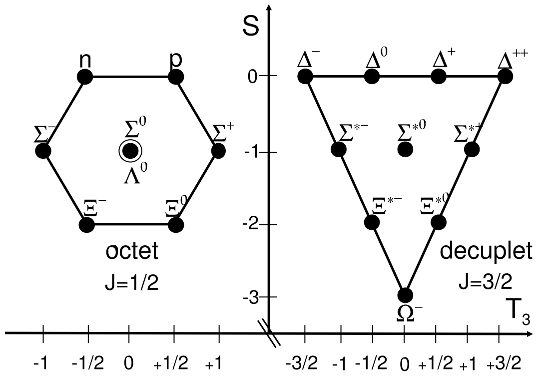

Fig. 1. SU(3) flavor octet and decuplet of ground-state baryons characterized by their strangeness S (vertical axis) and isospin component T_3 (horizontal axis).

Further considerations led Gell-Mann to propose that strong interactions conserve not only isospin and strangeness, but are also invariant under the higher SU(3) flavor symmetry [12] which ties isospin multiplets with different isospin T and strangeness S to larger degenerate multiplets of particles with the same spin $\mathbf{J}$ and parity P, e.g., to octets and decuplets (see Fig. 1). It was soon recognized that these higher multiplets emerge because baryons are composed of the same spin 1/2 flavor triplet quarks, which are merely coupled to a different total spin and flavor.

An even higher strong interaction symmetry is SU(6) spin-flavor symmetry, which unites the spin 1/2 flavor octet baryons (2×8 states), and the spin 3/2 flavor decuplet baryons (4×10 states) into a common **56**-dimensional mass degenerate supermultiplet [13,14]. There are numerous successful predictions based on SU(6) spin-flavor symmetry. For example, while SU(3) flavor symmetry alone does not suffice to uniquely determine the ratio of proton and neutron magnetic moments, SU(6) spin-flavor symmetry [14] leads to the prediction $\mu_p/\mu_n = -3/2$, which is in excellent agreement with the experimental result -1.46. Another example is the Gürsey-Radicati mass formula [13] which explains why the Gell-Mann Okubo mass formula works so well for both octet and decuplet baryons with the same numerical coefficients. Without an underlying spin-flavor symmetry this would remain mysterious.

Thus, SU(6) is a good symmetry in baryon physics, and the question arises whether it is a symmetry of quantum chromodynamics. In an $1/N_c$ expansion, where N_c denotes the number of colors, it has been shown that QCD possesses a spin-flavor symmetry which is exact in the large N_c limit [15,16]. For finite N_c, spin-flavor symmetry breaking operators can be classified according to the powers of $1/N_c$ associated with them. It turns out that higher orders of spin-flavor symmetry breaking are suppressed by correspondingly higher powers of $1/N_c$. This leads to a perturbative expansion scheme for QCD processes that works at all energy scales and provides a connection between broken SU(6) spin-flavor symmetry and the underlying quark-gluon dynamics [17,18].

3 Method

Alternatively, for $N_c = 3$ we may use a straightforward model-independent parametrization method developed by Morpurgo [19], which incorporates SU(6) symmetry and its breaking similar to the $1/N_c$ expansion. The basic idea is to *formally* define, for the observable at hand, a QCD operator Ω and QCD eigenstates $|B\rangle$ expressed explicitly in terms of quarks and gluons. The corresponding matrix element can, with the help of the unitary operator V, be reduced to an evaluation in the basis of auxiliary three-quark states $|\Phi_B\rangle$

$$\langle B|\Omega|B\rangle = \left\langle \Phi_B|V^\dagger \Omega V|\Phi_B\right\rangle = \langle W_B|\mathcal{O}|W_B\rangle \ . \qquad (1)$$

The auxiliary states $|\Phi_B\rangle$ are pure three-quark states with orbital angular momentum $L = 0$. The spin-flavor wave functions [20] contained in $|\Phi_B\rangle$ are denoted by $|W_B\rangle$. The operator V dresses the pure three-quark states with $q\bar{q}$ components and gluons and thereby generates the exact QCD eigenstates $|B\rangle$. Furthermore, it is implied that V contains a Foldy-Wouthuysen transformation allowing the auxiliary states to be written in terms of Pauli spinors.

One then writes the most general expression for the operator $\mathcal{O}$ that is compatible with the space-time and inner QCD symmetries. Generally, this is a sum of one-, two-, and three-quark operators in spin-flavor space multiplied by *a priori* unknown constants which parametrize the orbital and color space matrix elements. Empirically, a hierarchy in the importance of one-, two-, and three-quark operators is found. This fact can be understood in the $1/N_c$ expansion where two- and three-quark operators describing second and third order SU(6) symmetry breaking are usually suppressed by powers of $1/N_c$ and $1/N_c^2$ respectively, compared to one-quark operators associated with first order symmetry breaking. The method has been used to calculate various properties of baryons and mesons [19,21–23]. In the next section, we apply it to baryon charge radii and quadrupole moments.

4 Observables

Information on baryon structure is contained in the charge monopole form factor $G_{C0}(q^2)$, where q^2 is the four-momentum transfer of the virtual photon. In the Breit frame, the Fourier transform of $G_{C0}(q^2)$ corresponds to the charge density $\rho(r)$, describing the *radial* dependence of the baryon charge distribution. Its lowest radial moment is the baryon charge radius r_B^2.

However, the charge density need not be spherically symmetric, i.e., in general $\rho(\mathbf{r}) \neq \rho(r)$. The geometric shape of a baryon is determined by its intrinsic quadrupole moment [24], which can be inferred from the observable spectroscopic quadrupole moment Q_B. The latter corresponds to the charge quadrupole form factor $G_{C2}(q^2)$ at zero momentum transfer. For spin 1/2 baryons, which do not have a spectroscopic quadrupole moments due to angular momentum selection rules, one may still obtain information on their intrinsic quadrupole moments from measurements of electric ($E2$) and Coulomb ($C2$) quadrupole transitions to excited states [3].

The lowest moments of the charge density operator ρ are obtained from a multipole expansion at low momentum transfers. Up to q^2 contributions one has

$$\rho(q) = e - \frac{q^2}{6}\, r^2 - \frac{q^2}{6}\, \mathcal{Q} + \cdots \qquad (2)$$

The first two terms arise from the spherically symmetric monopole part, while the third term is obtained from the quadrupole part of ρ. They characterize the total charge (e), spatial extension (r^2), and shape ($\mathcal{Q}$) of the system.

4.1 Charge radii

According to the method outlined in the previous section, the charge radius operator can be expressed as a sum of one-, two-, and three-quark terms in spin-flavor space as

$$r^2 = A \sum_{i=1}^{3} e_i \mathbf{1} + B \sum_{i\neq j}^{3} e_i\, \boldsymbol{\sigma}_i \cdot \boldsymbol{\sigma}_j + C \sum_{i\neq j\neq k}^{3} e_k\, \boldsymbol{\sigma}_i \cdot \boldsymbol{\sigma}_j, \quad (3)$$

where $e_i = (1 + 3\tau_{i\,z})/6$ and $\boldsymbol{\sigma}_i$ are the charge and spin of the i-th quark. Here, $\tau_{i\,z}$ denotes the z component of the Pauli isospin matrix. These are the only allowed spin scalars that can be constructed from the generators of the spin-flavor group [25]. The constants A, B, and C parametrizing the orbital and color matrix elements are determined from experiment.

To estimate the degree of SU(3) flavor symmetry breaking we insert in Eq.(3) a linear and cubic quark mass dependence as

$$\mathbf{1} \rightarrow \mathbf{1}\ (m_u/m_s), \qquad \boldsymbol{\sigma}_i \cdot \boldsymbol{\sigma}_j \rightarrow \boldsymbol{\sigma}_i \cdot \boldsymbol{\sigma}_j\ m_u^3/(m_i^2 m_j). \quad (4)$$

Table 1. Baryon charge radii denoted by the particle symbols with one-quark (A), two-quark (B), and three-quark (C) contributions. Flavor symmetry breaking is characterized by the ratio of u-quark and s-quark masses $\zeta = m_u/m_s$. The flavor symmetry limit is obtained for $\zeta = 1$.

n	$-2B+4C$
p	$A-6C$
Σ^-	$[A(2+\zeta)+2(B+C)(1-2\zeta-2\zeta^2)]/3$
Σ^0	$[A(1-\zeta)+B(1-2\zeta+4\zeta^2)-2C(1+\zeta+\zeta^2)]/3$
Λ^0	$A(1-\zeta)/3-B+2C$
$\Lambda\Sigma$	$-\sqrt{3}(B\zeta-C(\zeta+\zeta^2))$
Σ^+	$[A(4-\zeta)+4B(1-2\zeta+\zeta^2)-2C(1+4\zeta+4\zeta^2)]/3$
Ξ^-	$[A(1+2\zeta)-2(B+C)(2\zeta+2\zeta^2-\zeta^3)]/3$
Ξ^0	$[A(2-2\zeta)-2B(4\zeta-2\zeta^2+\zeta^3)+4C(\zeta+\zeta^2+\zeta^3)]/3$
Δ^-	$A+2B+2C$
Δ^0	0
Δ^+	$A+2B+2C$
Δ^{++}	$A+2B+2C$
Σ^{*-}	$[A(2+\zeta)+2(B+C)(1+\zeta+\zeta^2)]/3$
Σ^{*0}	$[A(1-\zeta)+B(1+\zeta-2\zeta^2)-C(2-\zeta-\zeta^2)]/3$
Σ^{*+}	$[A(4-\zeta)+2B(2+2\zeta-\zeta^2)-2C(1-2\zeta-2\zeta^2)]/3$
Ξ^{*-}	$[A(1+2\zeta)+2(B+C)(\zeta+\zeta^2+\zeta^3)]/3$
Ξ^{*0}	$[A(2-2\zeta)+2B(2\zeta-\zeta^2-\zeta^3)-2C(\zeta+\zeta^2-2\zeta^3)]/3$
Ω^-	$A\zeta+2(B+C)\zeta^3$

These replacements are motivated by the different charge radii of up- and strange quarks and the flavor dependence of the gluon exchange current diagram [23]. Flavor symmetry breaking is then characterized by the ratio $\zeta = m_u/m_s$ of u and s quark masses. The latter is determined from the magnetic moment of the Λ hyperon. Our treatment of flavor symmetry breaking is not exact. Improvements are possible by introducing additional operators and constants in Eq.(3). However, there would then be so many undetermined constants that the theory can no longer make predictions. We expect that our approximate treatment of flavor symmetry breaking captures the most important physical effects. We use the same mass for u and d quarks to preserve the SU(2) isospin symmetry of the strong interaction that is known to hold to a very good accuracy.

Baryon charge radii are then calculated by evaluating matrix elements of the operator in Eq.(3) including the substitutions in Eq.(4) between three-quark spin-flavor wave functions $|W_B\rangle$

$$r_B^2 = \langle W_B|r^2|W_B\rangle. \quad (5)$$

For charged baryons, r_B^2 is normalized by dividing by the baryon charge. The results for octet and decuplet baryons are summarized in Table 1. The two- and three-quark results agree with those in Ref. [26] for $N_c = 3$ after obvious redefinition of the constants.

From Table 1 one readily observes that in the SU(6) symmetry limit all ground state baryons have the same charge radius $r_B^2 = A\,e$, where e is the baryon charge. In particular, the charge radii of the neutral baryons are zero. Inclusion of the spin-dependent two- and three-quark operators break SU(6) spin-flavor symmetry and split the charge radii of octet and decuplet baryons by decreasing the former and increasing the latter, e.g.

$$r^2_{\Sigma^{*-}} - r^2_{\Sigma^-} = r^2_{\Xi^{*-}} - r^2_{\Xi^-} = 2(B+C)(\zeta+\zeta^2) > 0. \quad (6)$$

Another consequence is that the neutral octet charge radii are definitely nonzero. If third order SU(6) symmetry breaking, i.e. the C term, can be neglected, the following relation holds [21,29]

$$r^2_{\Delta^+} - r^2_p = -r^2_n, \quad (7)$$

which shows that the octet-decuplet charge radius splitting is of the same order as the neutron charge radius.

Because there are 19 experimental charge radii (8 diagonal octet, 1 transition octet, and 10 diagonal decuplet) and 3 constants, Table 1 contains 16 relations among the baryon charge radii, some of which are independent of the SU(3) symmetry breaking parameter ζ and thus hold irrespective of how badly SU(3) flavor symmetry is broken. An example of the latter type is the Σ equal spacing rule,

$$r^2_{\Sigma^+} - r^2_{\Sigma^-} = 2\,r^2_{\Sigma^0}, \qquad r^2_{\Sigma^{*+}} - r^2_{\Sigma^{*-}} = 2\,r^2_{\Sigma^{*0}}, \quad (8)$$

which is already a consequence of the assumed isospin symmetry. Another example is the equal spacing rule for decuplet charge radii

$$3\,(r^2_{\Xi^{*-}} - r^2_{\Sigma^{*-}}) = r^2_{\Omega^{*-}} - r^2_{\Delta^{*-}}, \quad (9)$$

which the reader may easily verify using Table 1. Analogous relations hold for baryon quadrupole moments [23].

To make numerical predictions, we express the three parameters A, B, and C in Eq.(3) in terms of the three measured charge radii r_p^2, r_n^2, and $r^2_{\Sigma^-}$ using the results in Table 1

$$A(3-\zeta-2\zeta^2) = (1-2\zeta-2\zeta^2)(r_p^2 - r_n^2) + 3r^2_{\Sigma^-},$$
$$-3B(3-\zeta-2\zeta^2) = (2+\zeta)r_p^2 + \frac{1}{2}(7+\zeta-2\zeta^2)r_n^2 - 3\,r^2_{\Sigma^-},$$
$$-6C(3-\zeta-2\zeta^2) = (2+\zeta)r_p^2 - \frac{1}{2}(2-4\zeta-4\zeta^2)r_n^2 - 3r^2_{\Sigma^-}.$$

With the experimental radii and $\zeta = 0.613$ we obtain $A = 0.723$ fm^2, $B = 0.039$ fm^2, $C = -0.009$ fm^2 and the numerical results shown in Table 2 (a). For comparison, we also use $r^2_{\Sigma^-} = 0.64(0.67)$ fm^2 as input, which leads to $A = 0.779(0.873)$ fm^2, $B = 0.058(0.077)$ fm^2, $C = 0(0.010)$ fm^2, and the results labelled (b) and (c) in Table 2. Thus, while the constant $B > 0$ is fixed by the negative neutron charge radius, the sign of C cannot be reliably determined. In any case, the C term is definitely smaller than the B term by at least a factor of $1/N_c$.

Table 2 shows that octet baryon charge radii are ordered as $r^2_{\Sigma^+} > r^2_p > r^2_{\Sigma^-} > r^2_{\Xi^-}$. For decuplet baryons one finds $r^2_{\Sigma^{*+}} > r^2_{\Delta^+} > r^2_{\Sigma^{*-}} > r^2_{\Xi^{*-}} > r^2_{\Omega^-}$. In both flavor multiplets the decrease in each step is of order $|r_n^2|$. Note that only r_n^2 and $r^2_{\Lambda\Sigma}$ are negative [30]. With respect to the size of SU(6) symmetry breaking, we obtain for the parameter sets (a)-(c) a relative charge radius splitting $(r^2_{\Delta^+} - r^2_p)/[(r^2_{\Delta^+} + r^2_p)/2]$ of 0.5%, 14%, and 26%. For $r^2_{\Sigma^-} = 0.91(36)$ fm^2 [6] (WA89 experiment) the splitting would be 83%, which is too large, if the relative octet-decuplet splitting for charge radii and masses is similar, as we expect.

Table 2. Numerical charge radii in [fm^2] according to Table 1. We use the measured charge radii $r_n^2 = -0.1161(22)$ fm^2 [27], $r_p^2 = 0.779(25)$ fm^2 [28], and $\zeta = 0.613$ as input. Three different values for $r^2_{\Sigma^-}$ are used as input: $r^2_{\Sigma^-} = 0.61(21)$ fm^2 [6] (a), $r^2_{\Sigma^-} = 0.64$ fm^2 (b), and $r^2_{\Sigma^-} = 0.67$ fm^2 (c).

	(a)	(b)	(c)
n	-0.116	-0.116	-0.116
p	0.779	0.779	0.779
Σ^-	0.610	0.641	0.672
Σ^0	0.122	0.125	0.128
Λ^0	0.035	0.043	0.050
$\Lambda^0\Sigma^0$	-0.058	-0.062	-0.066
Σ^+	0.855	0.891	0.928
Ξ^-	0.501	0.510	0.520
Ξ^0	0.120	0.126	0.132
Δ^-	0.783	0.895	1.011
Δ^0	0	0	0
Δ^+	0.783	0.895	1.011
Δ^{++}	0.783	0.895	1.011
Σ^{*-}	0.669	0.756	0.845
Σ^{*0}	0.108	0.117	0.127
Σ^{*+}	0.869	0.988	1.086
Ξ^{*-}	0.561	0.625	0.692
Ξ^{*0}	0.206	0.225	0.244
Ω^-	0.457	0.504	0.553

Table 3. Transition and diagonal baryon quadrupole moments denoted by the particle symbols with two-quark (B') and three-quark (C') contributions. From Ref. [23].

$n \to \Delta^0$	$2\sqrt{2}(B' - 2C')$
$p \to \Delta^+$	$2\sqrt{2}(B' - 2C')$
$\Sigma^- \to \Sigma^{*-}$	$-\sqrt{2}\,(2B' + 2C')\,(2-\zeta-\zeta^2)/3$
$\Sigma^0 \to \Sigma^{*0}$	$\sqrt{2}[2B'(2-\zeta+2\zeta^2) - 2C'(4+\zeta+\zeta^2)]/6$
$\Lambda^0 \to \Sigma^{*0}$	$\sqrt{6}[2B'\zeta - 2C'(\zeta+\zeta^2)]/2$
$\Sigma^+ \to \Sigma^{*+}$	$2\sqrt{2}\,[B'\,(4-2\zeta+\zeta^2) - 2C'\,(1+\zeta+\zeta^2)]/3$
$\Xi^- \to \Xi^{*-}$	$-\sqrt{2}\,(2B'+2C')\,(\zeta+\zeta^2-2\zeta^3)/3$
$\Xi^0 \to \Xi^{*0}$	$\sqrt{2}[2B'(2\zeta-\zeta^2+2\zeta^3) - 2C'(\zeta+\zeta^2+4\zeta^3)]/3$
Δ^-	$-4B' - 4C'$
Δ^0	0
Δ^+	$4B' + 4C'$
Δ^{++}	$8B' + 8C'$
Σ^{*-}	$-(4B'+4C')(1+\zeta+\zeta^2)/3$
Σ^{*0}	$[2B'(1+\zeta-2\zeta^2) - 2C'(2-\zeta-\zeta^2)]/3$
Σ^{*+}	$[4B'(2+2\zeta-\zeta^2) - 4C'(1-2\zeta-2\zeta^2)]/3$
Ξ^{*-}	$-(4B'+4C')(\zeta+\zeta^2+\zeta^3)/3$
Ξ^{*0}	$[4B'(2\zeta-\zeta^2-\zeta^3) - 4C'(\zeta+\zeta^2-2\zeta^3)]/3$
Ω^-	$-(4B'+4C')\zeta^3$

4.2 Quadrupole moments

The charge quadrupole operator is composed of a two- and three-body term in spin-flavor space

$$\mathcal{Q} = B' \sum_{i\neq j}^{3} e_i\,(3\sigma_{i\,z}\sigma_{j\,z} - \boldsymbol{\sigma}_i\cdot\boldsymbol{\sigma}_j) + C' \sum_{i\neq j\neq k}^{3} e_k\,(3\sigma_{i\,z}\sigma_{j\,z} - \boldsymbol{\sigma}_i\cdot\boldsymbol{\sigma}_j)\,. \tag{10}$$

Table 4. Numerical quadrupole moments in [fm^2] according to Table 3 using the parameter sets (a)-(c) of sect. 4.1.

	(a)	(b)	(c)
$n \to \Delta^0$	-0.082	-0.082	-0.082
$p \to \Delta^+$	-0.082	-0.082	-0.082
$\Sigma^- \to \Sigma^{*-}$	0.014	0.028	0.042
$\Sigma^0 \to \Sigma^{*0}$	-0.031	-0.029	-0.028
$\Lambda^0 \to \Sigma^{*0}$	-0.041	-0.044	-0.046
$\Sigma^+ \to \Sigma^{*+}$	-0.076	-0.086	-0.097
$\Xi^- \to \Xi^{*-}$	0.007	0.014	0.022
$\Xi^0 \to \Xi^{*0}$	-0.033	-0.036	-0.039
Δ^-	0.060	0.116	0.174
Δ^0	0	0	0
Δ^+	-0.060	-0.116	-0.174
Δ^{++}	-0.120	-0.232	0.348
Σ^{*-}	0.039	0.077	0.115
Σ^{*0}	0.014	-0.017	-0.019
Σ^{*+}	-0.069	-0.110	-0.153
Ξ^{*-}	0.024	0.047	0.071
Ξ^{*0}	-0.019	-0.023	-0.029
Ω^-	0.014	0.027	0.040

Baryon decuplet quadrupole moments Q_{B^*} and octet-decuplet transition quadrupole moments $Q_{B\to B^*}$ are obtained by calculating the matrix elements of the quadrupole operator in Eq.(10) between the three-quark spin-flavor wave functions $|W_B\rangle$

$$Q_{B^*} = \langle W_{B^*}|\mathcal{Q}|W_{B^*}\rangle\,, \quad Q_{B\to B^*} = \langle W_{B^*}|\mathcal{Q}|W_B\rangle\,, \tag{11}$$

where B denotes a spin 1/2 octet baryon and B^* a member of the spin 3/2 baryon decuplet. The ensuing quadrupole moment relations have been discussed earlier [23]. Table 3 reproduces the main results.

Interestingly, SU(6) symmetry does not only lead to charge radius and quadrupole moment relations, but also furnishes relations between both sets of observables [31, 32]. This can be seen from a comparison of Table 1 and Table 3 using the relations $B' = -B/2$ and $C' = -C/2$ [33]. For example, we find that the $N \to \Delta$ quadrupole moment is related to the neutron charge radius as [29]

$$Q_{p\to\Delta^+} = Q_{n\to\Delta^0} = \frac{1}{\sqrt{2}}\,r_n^2, \tag{12}$$

which is experimentally well satisfied [34]. This relation also holds for the corresponding form factors up to momentum transfers in the GeV region [32]. In the SU(3) symmetry limit, the transition quadrupole moments of nonnegative hyperons are proportional to r_n^2, as can be verified from Tables 1 and 3 for $\zeta = 1$. Thus, the neutron charge radius plays an important role. It sets the scale not only for the charge radius splitting within and between flavor multiplets but also for the size of quadrupole moments and the corresponding intrinsic baryon deformation [24, 31,32]. Another example of the predictive power of SU(6) spin-flavor symmetry is the Ω^- quadrupole moment

$$Q_{\Omega^-} = \frac{1}{3-\zeta-2\zeta^2}\,\left(3\,r^2_{\Sigma^-} - (2+\zeta)\,(r_p^2 + r_n^2)\right)\zeta^3, \tag{13}$$

which has been expressed here in terms of the three measured baryon charge radii. Finally, Table 4 provides numerical predictions for baryon quadrupole moments using parameter sets (a)-(c) of sect. 4.1.

5 Summary

We have calculated baryon charge radii and quadrupole moments using a parametrization method based on the symmetries of QCD, and derived a number of charge radius and quadrupole moment relations. In addition, SU(6) symmetry leads to interesting relations between these two sets of observables. Using the three measured radii as input, we have obtained numerical predictions for the remaining charge radii and baryon quadrupole moments. Our results suggest that one can obtain information on the shape of baryons both from quadrupole moment and charge radius measurements.

References

1. G. D. Rochester and C. C. Butler, Nature **160** (1947) 855.
2. M. K. Jones, Phys. Rev. Lett. **84** (2000) 1398; O. Gayou, Phys. Rev. Lett. **88** (2002) 092301.
3. A.M. Bernstein, Eur. Phys. J. **A 17** (2003) 349; C.N. Papanicolas, Eur. Phys. J. **A 18** (2003) 141.
4. J.J. Kelly, Phys. Rev. C **66** (2002) 065203.
5. E. E. Chambers and R. Hofstadter, Phys. Rev. **103** (1956) 1454; E. Fermi and L. Marshall, Phys. Rev. **72** (1947) 1139; L. L. Foldy, Phys. Rev. **87** (1952) 693.
6. I. Eschrich et al., Phys. Lett. B**522** (2001) 233; M.I. Adamovich et al., Eur. Phys. C **8** (1999) 59. The Σ^- is the only strange baryon whose charge radius has been measured.
7. It is planned to measure the Ω^- quadrupole moment with the Panda detector at GSI in Darmstadt: J. Pochodzalla, Nucl. Instr. Meth. B **214** (2004) 149.
8. J. Kunz and P. J. Mulders, Phys. Rev. D **41** (1990) 1578; N. Barik, S. N. Jena, D. P. Rath, Phys. Rev. D **41** (1990) 1568; B. Povh and J. Hüfner, Phys. Lett. B **245** (1990) 653; Georg Wagner, A. J. Buchmann, and A. Faessler, Phys. Rev. C **58** (1998) 3666; E. J. Hackett-Jones, D. B. Leinweber, A. W. Thomas, Phys. Lett. B **494** (2000) 89; S. J. Puglia, M. J. Ramsey-Musolf, and Shi-Lin Zhu, Phys. Rev. D **63** (2001) 034014; D. Arndt and B. C. Tiburzi, Phys. Rev. D **68** (2003) 114503.
9. Y. Oh, Mod. Phys. Lett. A **10** (1995) 1027; J. Kroll, B. Schwesinger, Phys. Lett. B **334** (1994) 287; J. M. Richard, Z. Phys. C **12** (1982) 369; M. I. Krivoruchenko, M. M. Giannini, Phys. Rev. D **43** (1990) 3763; M. N. Butler, M. J. Savage, R. P. Springer, Phys. Rev. D **49** (1994) 3459; G. Karl and V. A. Novikov, Phys. Rev. C **74** (2006) 024001.
10. For an excellent summary see: Abraham Pais, *Inward Bound* (Oxford University Press, Oxford 1986)
11. M. Gell-Mann, Phys. Rev. **92** (1953) 833; T. Nakano and K. Nishijima, Prog. Theor. Phys. **10** (1953) 581; A. Pais, Phys. Rev. **86** (1952) 663.
12. M. Gell-Mann and Y. Ne'eman, The Eightfold Way, W. A. Benjamin, New York 1964.
13. F. Gürsey and L.A. Radicati, Phys. Rev. Lett. **13** (1964) 173; B. Sakita, Phys. Rev. Lett. **13** (1964) 643.
14. M.A.B. Beg, B.W. Lee, and A. Pais, Phys. Rev. Lett. **13** (1964) 514.
15. J.-L. Gervais and B. Sakita, Phys. Rev. D **30** (1984) 1795.
16. R.F. Dashen, E. Jenkins, and A.V. Manohar, Phys. Rev. D **51** (1995) 3697.
17. E. Witten, Nucl. Phys.**B160** (1979) 57.
18. For a summary see: R.F. Lebed, Czech. J. Phys. **49** (1999) 1273; nucl-th/9810080.
19. G. Morpurgo, Phys. Rev. D **40** (1989) 2997.
20. D. B. Lichtenberg, Unitary Symmetry and Elementary Particles, Academic Press, New York, 1978; F. E. Close, An introduction to Quarks and Partons, Academic Press, London, 1979.
21. G. Dillon and G. Morpurgo, Phys. Lett. B **448** (1999) 107.
22. G. Dillon and G. Morpurgo, Europhys. Lett. **54** (2001) 35.
23. A.J. Buchmann and E.M. Henley, Phys. Rev. D**65** (2002) 073017. In Tables 1 and 2, the constant C should be replaced by $2\,C$. This does not affect any of the relations or numerical results. In Table 2, second column, fourth row, the factor of 2 should not be there. In Table 4, second column, fourth row, replace -0.08 by -0.04. In Eq.(8d) replace r^3 by $2\,r^3$.
24. A. J. Buchmann and E.M. Henley, Phys. Rev. C **63** (2001) 015202. The intrinsic quadrupole moment is connected with, but generally not identical to the spectroscopic quadrupole moment.
25. A. J. Buchmann and R. F. Lebed, Phys. Rev. D **62** (2000) 096005. The error made by omitting operators containing second and third orders of e_i is negligble.
26. A.J. Buchmann and R. F. Lebed, Phys. Rev. D **67** (2003) 016002.
27. S. Eidelman et al., Phys. Lett. B **522** (2001) 233.
28. R. Rosenfelder, Phys. Lett. B **479** (2000) 381.
29. A.J. Buchmann, E. Hernández, A. Faessler, Phys. Rev. C **55** (1997) 448.
30. In contrast to Ref. [26] we predict here $r^2_\Lambda > 0$. This is due to our inclusion of SU(3) flavor symmetry breaking in the one-quark term in Eq.(3).
31. A. J. Buchmann, Proceedings of the Shape of Hadrons Workshop, Athens, Greece, 27-29 April 2006, edited by C. N. Papanicolas and A. M. Bernstein (AIP).
32. A.J. Buchmann, Phys. Rev. Lett. **93** (2004) 212301.
33. In SU(6), the spin scalar charge radius and spin tensor quadrupole moment operators are related [31].
34. L. Tiator, D. Drechsel, S.S. Kamalov, and S. N. Yang, Eur. Phys. J. **A17** (2003) 357, Blanpied et al., Phys. Rev. C **64**, (2001) 025203.